

Sat2RealCity: Geometry-Aware and Appearance-Controllable 3D Urban Generation from Satellite Imagery

Yijie Kang* Xinliang Wang* Zhenyu Wu Yifeng Shi† Hailong Zhu
Ke Holdings Inc.

{kangyijie001, wangxinliang008, wuzhenyu018, shiyifeng003, zhuhailong016}@ke.com

Abstract

Recent advances in generative modeling have substantially enhanced 3D urban generation, enabling applications in digital twins, virtual cities, and large-scale simulations. However, existing methods face two key challenges: (1) the need for large-scale 3D city assets for supervised training, which are difficult and costly to obtain, and (2) reliance on semantic or height maps, which are used exclusively for generating buildings in virtual worlds and lack connection to real-world appearance, limiting the realism and generalizability of generated cities. To address these limitations, we propose *Sat2RealCity*, a geometry-aware and appearance-controllable framework for 3D urban generation from real-world satellite imagery. Unlike previous city-level generation methods, *Sat2RealCity* builds generation upon individual building entities, enabling the use of rich priors and pretrained knowledge from 3D object generation while substantially reducing dependence on large-scale 3D city assets. Specifically, (1) we introduce the OSM-based spatial priors strategy to achieve interpretable geometric generation from spatial topology to building instances; (2) we design an appearance-guided controllable modeling mechanism for fine-grained appearance realism and style control; and (3) we construct a MLLM-powered semantic-guided generation pipeline, bridging semantic interpretation and geometric reconstruction. Extensive quantitative and qualitative experiments demonstrate that *Sat2RealCity* significantly surpasses existing baselines in structural consistency and appearance realism, establishing a strong foundation for real-world-aligned 3D urban content creation. The code will be released soon.

1. Introduction

In recent years, generative modeling has made remarkable progress in visual content creation, extending from 2D image generation [34, 44, 51] to 3D generation [25, 31, 43,

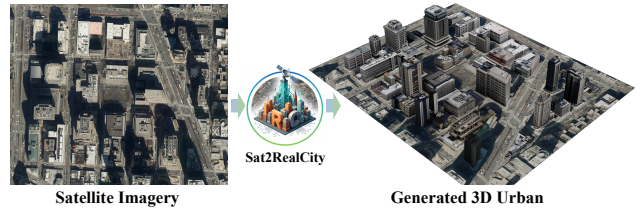


Figure 1. We present *Sat2RealCity*, a novel framework for generating high-fidelity 3D city models with detailed geometry and appearance from real-world satellite imagery.

49]. Such advances have opened up new opportunities for constructing digital twins, virtual cities, and large-scale simulation environments. In particular, 3D urban generation is the task of producing realistic and structurally consistent 3D city scenes and has attracted growing attention due to its potential in urban planning, autonomous driving, and geographic visualization [5, 10, 22, 27, 28, 36, 45]. Despite rapid progress, existing 3D city generation approaches still face two fundamental challenges. First, they typically rely on large-scale 3D city assets for supervised training [10, 26], yet such datasets are extremely scarce and expensive to obtain, as manual modeling and georeferenced alignment are costly and time-consuming. Moreover, most available datasets are captured at the tile level rather than representing complete, city-scale scenes, leading to limited spatial continuity and constraining the scalability of generation across larger urban regions. Second, most methods depend on simplified inputs such as semantic maps or height maps [6, 22, 36], which fail to capture the fine-grained appearance, material, and structural details of real-world cities. As a result, the generated content often lacks realism and generalizability when deployed in real-world contexts.

In order to overcome these drawbacks, we propose *Sat2RealCity*, a geometry-aware and appearance-controllable framework for 3D urban generation directly from real-world satellite imagery. Unlike previous city-level generation methods that treat entire urban blocks as monolithic scenes, *Sat2RealCity* operates at the building-entity level, allowing fine-grained control and the incorpo-

*Equal contribution † Corresponding author

ration of rich priors from pretrained 3D object generation models. This design substantially reduces the dependence on large-scale 3D city assets while enhancing structural interpretability and appearance fidelity. Our main contributions are summarized as follows:

- **OSM-based spatial priors.** We introduce interpretable geometric priors that guide building-wise 3D generation from spatial topology to instance-level geometry.
- **Appearance-guided controllable modeling.** This mechanism enables fine-grained control over texture synthesis, ensuring realistic appearance and consistency in generated 3D urban scenes while allowing style customization.
- **MLLM-powered semantic-guided generation.** Leveraging multimodal reasoning, this pipeline enhances both semantic understanding and visual realism, ensuring that generated structures align more faithfully with real-world context while maintaining coherent appearance across diverse urban regions.
- **Comprehensive evaluation.** Extensive experiments on multiple real-world regions demonstrate that Sat2RealCity achieves superior geometric faithfulness, appearance realism, and cross-region consistency compared to existing methods.

By unifying semantic, geometric, and visual cues from satellite imagery, Sat2RealCity lays the foundation for scalable, real-world-aligned 3D urban content creation.

2. Related Work

2.1. 3D Object Generation

The field of 3D content generation has seen rapid development in recent years. Early research generate 3D objects by leveraging powerful 2D priors [24, 25, 31], most notably with Score Distillation Sampling (SDS) introduced by DreamFusion [31]. However, this optimization-based paradigm suffers from inherent flaws: generation is extremely slow, gradients are unstable, and it often results in view-inconsistency and low-quality geometry. To achieve efficient feed-forward generation [9, 38, 46, 48, 50], the community has explored two dominant paths for 3D latent representations. The first path relies on vector-set (VecSet) representations [16, 17, 19, 21, 39, 40, 52], as shown in 3DShape2VecSet [49]. It encodes a 3D shape as an unordered set of vectors, which is naturally suited for Transformer architectures and enables powerful global relationship modeling. Another research line focuses on the Voxel-VAE paradigm, including works such as XCube [33], TRELIS [43] and SparseFlex [8]. While these methods generate individual objects or views, generating complete, structured, and real-world-aligned 3D urban scenes from satellite imagery remains challenging. Sat2RealCity extends the entity-level generation idea, inspired by direct 3D generation’s goal of scene structure but addressing its

data limitations by leveraging satellite inputs and appearance control, bridging the gap between single-object generation and scalable urban creation.

2.2. 3D Urban Generation

3D urban generation aims to synthesize city-scale scenes with realistic geometry and appearance, supporting applications such as urban planning, simulation, and virtual reality. One category of methods employs procedural or rule-based techniques [5, 53], which can generate structured city layouts but lack diversity and fine-grained realism. Another category focuses on data-driven approaches leveraging semantic or height maps to reconstruct building geometry [22, 36]. While effective at generating coarse city blocks, these methods often ignore real-world appearance, limiting visual fidelity and generalizability. A further line of work incorporates multi-modal priors, where geospatial datasets and learned 3D priors are used to produce more realistic layouts [6, 10]. These methods still treat scenes holistically and are constrained by availability of large 3D assets. Image-guided generation approaches enable control over urban textures or style [26], yet maintaining structural consistency across large-scale regions remains challenging. In contrast, Sat2RealCity adopts a building-entity-based generation paradigm, combining interpretable geometric priors, appearance control, and semantic guidance. This design allows fine-grained, scalable 3D urban synthesis directly from satellite imagery, bridging the gap between single-object generation and city-scale reconstruction while achieving both geometric fidelity and visual realism.

3. Method

3.1. Preliminary

TRELIS. We chose TRELIS [43] as the starting point for our method because TRELIS provides a powerful generative prior and has shown great potential in the field of 3D object generation. It adopts a two-stage generation process. In the first stage, it generates a sparse structure $\{p_i\}_{i=1}^L$ via SS Flow, where p_i is the localization index of an activated voxel in the 3D voxel grid that intersects with the 3D asset’s surface. In the second stage, it generates a structured latent $z = \{(z_i, p_i)\}_{i=1}^L$ via SLAT Flow. Subsequently, z can be decoded into multiple 3D representations, including NeRF [29], 3DGS [13], and Mesh.

Both stages of generation utilize rectified flow transformers, accepting image features encoded by DINOv2 [30] as conditional injection. The rectified flow model uses a linear interpolation forward process $\mathbf{x}(t) = (1 - t)\mathbf{x}_0 + t\epsilon$, which interpolates between data samples \mathbf{x}_0 and noises ϵ with a timestep t , and the backward process is represented as a vector field $\mathbf{v}(\mathbf{x}, t) = \nabla_t \mathbf{x}$. The two-stage model \mathbf{v}_θ fits this vector field by minimizing the Conditional Flow

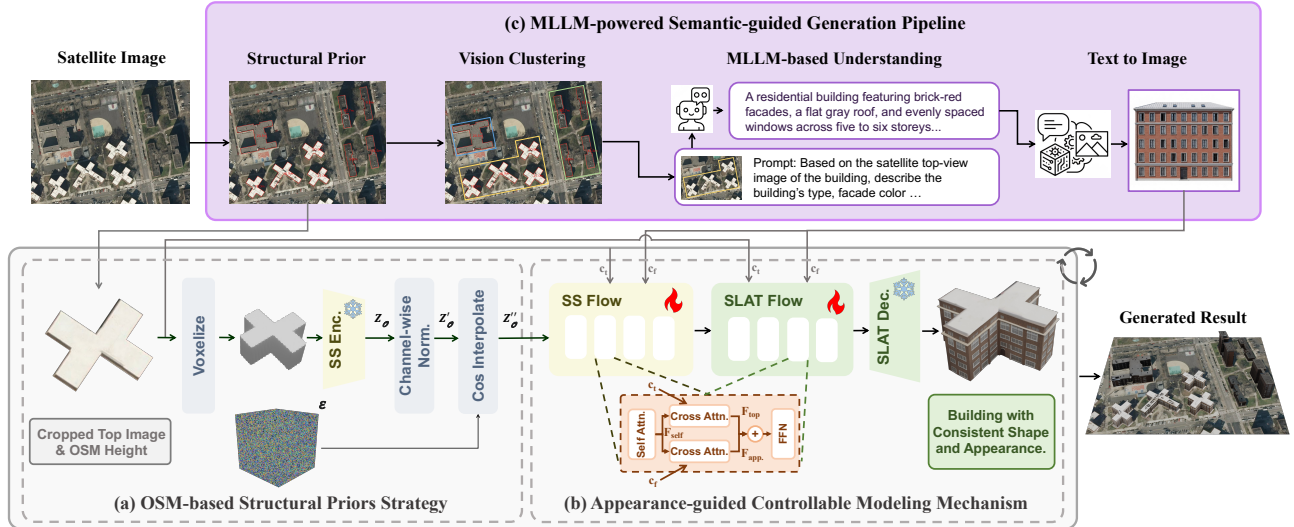


Figure 2. **The overview of Sat2RealCity.** (a) The **OSM-based Structural Priors Strategy** converts OSM data into a fused geometric prior Z''_O . (b) The **Appearance-guided Modeling Mechanism** uses Z''_O , the top view feature c_t , and a frontal appearance image feature c_f to generate the 3D building. (c) The **MLLM-powered Generation Pipeline** provides geometric priors and the frontal-view image for modules (a) and (b). Finally, all generated buildings are assembled into the urban scene using their original OSM coordinates.

Matching (CFM) objective:

$$\mathcal{L}_{CFM}(\theta) = \mathbb{E}_{t, \mathbf{x}_0, \epsilon} \|\mathbf{v}_\theta(\mathbf{x}, t) - (\epsilon - \mathbf{x}_0)\|_2^2. \quad (1)$$

Overview. The goal of Sat2RealCity is to generate realistic and semantically consistent 3D urban scenes directly from real-world satellite imagery. To address the challenges faced by existing city-generation methods, namely the difficulty of collecting large-scale 3D urban assets for supervised training and the domain gap between virtual and real-world appearance, we design a geometry-aware and appearance-controllable generation framework, as illustrated in Figure 2.

Instead of relying on city-scale 3D datasets that are costly and labor-intensive to construct, we focus on building-entity-based generation, where individual building assets are learned and composed into realistic urban scenes. To this end, we build a dedicated 3D Building Dataset, which contains a diverse collection of modern-style buildings synthesized through a text-to-image-to-3D pipeline. Compared with large-scale urban reconstructions, creating such building-level 3D assets is significantly more feasible while still providing rich geometric and appearance supervision for model training.

Inspired by the two-stage structure-and-appearance generation paradigm in TRELIS [43], our framework first employs an OSM-guided structural priors strategy integrating spatial topology and building-height information extracted from satellite imagery and OSM data to produce geometry-aware urban layouts. Subsequently, appearance-guided controllable modeling mechanism leverages build-

ing appearance condition image (i.e., frontal-view) to guide the visual style of each building. This process is realized via an MLLM-powered semantic-guided generation pipeline, which provides OSM priors during inference and generates appearance control maps using the multimodal model’s understanding capabilities. Afterward, individual building entities are placed according to centroid positions specified by the OSM priors, completing the 3D urban scene generation process. This coordinated pipeline enables Sat2RealCity to achieve high-fidelity, real-world-aligned 3D urban generation without relying on large-scale 3D city datasets.

3.2. 3D Building Dataset

While several large-scale 3D datasets such as Objaverse-XL [4], ABO [3], HSSD [14], and 3D-FUTURE [7] have recently emerged, none provide a dedicated, high-quality corpus of 3D building assets. Existing collections contain few architectural models, often of limited fidelity [1, 11, 18, 41, 42] and stylistic variety [23].

To bridge this gap and enable fine-tuning for satellite-guided 3D building generation, we constructed a dataset of 11,579 high-quality, AIGC-generated building models. The dataset spans diverse architectural categories with rich attributes and detailed geometry, and **will be released as an open-source resource for the community.**

The dataset is constructed through two main stages: Systematic Text Prompt Generation and Image and 3D Asset Generation, which are detailed below.

Systematic Text Prompt Generation. We designed a hierarchical prompt generator with two key components: a structured library of building descriptors (e.g., function,



Figure 3. Examples of the 3D Building Dataset.

style, wall material, roof type) and a rule-based combination scheme. A depth-first search (DFS) traverses the component tree, filtering incompatible attribute combinations (e.g., excluding glass curtain walls for industrial buildings) to ensure semantic and structural coherence. Each generated prompt is validated by a large language model for naturalness and plausibility, followed by deduplication to ensure uniqueness. The complete logic graph of building construction is provided in the supplementary material.

Image and 3D Asset Generation. Validated prompts are fed into Google Imagen 4 to synthesize corresponding building images. The two-step image-first approach leverages the high fidelity of text-to-image models to provide a strong visual prior for 3D lifting. The generated images are refined with a diffusion-based cleanup model to remove irrelevant artifacts (e.g., pedestrians, vegetation, road surfaces). Finally, the cleaned images are converted into 3D assets using Hunyuan3D 2.5 [16], producing a diverse and high-quality dataset tailored for 3D building generation research. Representative 3D assets from our dataset are shown in Figure 3.

3.3. OSM-based Structural Priors for Geometry-Aware and Geospatial Alignment

Generating 3D buildings directly from a single top-down satellite image is inherently ambiguous: the image conveys appearance and coarse 2D structure but lacks explicit cues for building height, fine-grained geometry, and global orientation. To achieve geometry-aware and geospatially aligned generation, we propose the **OSM-based structural priors strategy**, which introduces structural priors derived from OpenStreetMap (OSM) as explicit geometric guidance, as shown in Figure 2(a).

We first extrude OSM building footprints into coarse volumetric proxies, which are obtained from a downsampled version of a 3D asset voxel during training, and encode them into a Sparse Structure (SS) latent space using pretrained Sparse Structure VAE encoder [43], yielding the prior latent $Z_{\mathcal{O}}$. A channel-wise normalization (SS Latent Norm) is applied to align the latent distribution with a Gaussian prior, producing $Z'_{\mathcal{O}}$. To balance deterministic geomet-

ric cues with generative stochasticity, we perform Cosine Geometric Interpolation between $Z'_{\mathcal{O}}$ and Gaussian noise $\epsilon \sim \mathcal{N}(0, I)$:

$$Z''_{\mathcal{O}} = \cos\left(\frac{\lambda\pi}{2}\right) Z'_{\mathcal{O}} + \sin\left(\frac{\lambda\pi}{2}\right) \epsilon, \quad (2)$$

where λ is a hyperparameter that controls the strength of the structural prior. The fused latent $Z''_{\mathcal{O}}$ serves as the initialization for the SS Flow Transformer, replacing the pure noise input used in conventional diffusion-based 3D generators. During training, we randomly sample among multiple Levels of Detail (LODs) of OSM-derived geometry—such as LOD 0 (bounding boxes) and LOD 1 (extruded footprints)—and pair them with different noise intensities. This stochastic sampling prevents overfitting to specific priors and enhances generalization to diverse urban morphologies.

In contrast to Sat-Skylines [12], which employs structural priors mainly for coarse shape and height conditioning, our method leverages an implicit but crucial advantage: joint geometry-aware and geospatial alignment. Because OSM footprints are geospatially registered with satellite imagery, the encoded latent inherently captures both absolute orientation and structural cues, including building contour, aspect ratio, and relative elevation, within a unified top-down coordinate frame. Consequently, our model learns to generate 3D structures that are not only automatically aligned with their real-world positions and rotations but also structurally faithful to the underlying urban morphology.

This design enables Sat2RealCity to directly produce large-scale, geometry-aware and spatially consistent 3D urban scenes, where every generated building precisely matches its satellite footprint in both geometric structure and geospatial pose.

3.4. Appearance-guided Controllable Modeling for Regional Stylistic Consistency

While the OSM-based structural priors strategy enforce geometric and pose alignment for individual buildings, generating realistic urban scenes requires maintaining regional stylistic consistency. In real cities, buildings within the same neighborhood or complex often share common architectural characteristics, such as facade materials, color tones, and window layouts—despite variations in their footprints or heights. Generating each building independently from its own top-view image leads to excessive appearance variance, producing visually fragmented and unrealistic results.

To address this, we introduce an **appearance-guided controllable modeling mechanism** that enables a group of buildings to share a unified style while preserving their geometry, as illustrated in Figure 2(b). During inference, we assign a shared appearance condition image (i.e., front-view) to all buildings within a region, ensuring a cohesive

stylistic appearance aligned with their individual satellite-derived structures.

We propose parallel cross-attention pathways, which are incorporated within each SS Flow and SLAT Flow transformer block, following the self-attention and preceding the feed-forward network (FFN), as illustrated in Figure 2:

- **Structure Pathway:** conditioned on the top (satellite) image, which is rendered from a top view of the 3D asset during training and cropped from real satellite imagery based on OSM footprints during inference, enforcing geometric fidelity and spatial alignment. Formulated as:

$$F_{top} = CrossAttn(Q(F_{self}, K(c_t), V(c_t))); \quad (3)$$

- **Appearance Pathway:** conditioned on a frontal image, which is rendered from a frontal view of the 3D asset during training and generated by our MLLM-based pipeline (Sec. 3.5) during inference, guiding stylistic coherence across buildings. Formulated as:

$$F_{appearance} = CrossAttn(Q(F_{self}, K(c_f), V(c_f))), \quad (4)$$

where F_{self} is the output of the self-attention layer, c_t and c_f are respectively the top view and the frontal-view DINOv2 [30] feature, $Q(\cdot)$, $K(\cdot)$ and $V(\cdot)$ are linear layers respectively for query, key and value projection. To preserve the pretrained capacity of the foundation model, the weights of the both pathway cross-attention are initialized from the pretrained weights. The outputs of both pathways, F_{top} and $F_{appearance}$, are fused by simple element-wise averaging before being passed to the FFN.

This design yields a powerful and highly desirable disentanglement of control. We hypothesize this efficacy stems from the spatial nature of the Structured Latent (SLAT) representation [43]. The transformer blocks operate on sparse latents (z_i, p_i) , where p_i provides explicit 3D positional information. The averaging fusion provides the FFN with two ‘‘opinions’’ simultaneously. The model learns a **spatially-dependent policy** to utilize this fused signal:

- For localization index p_i corresponding to the **roof**, the signal from the top-view (F_{top}) is highly relevant and is thus prioritized.
- For localization index p_i corresponding to **facades/walls**, the signal from the frontal-view ($F_{appearance}$) is more informative and is therefore prioritized.

This learned, selective utilization precisely enables our core application: the model can resolve competing signals by applying *unique* geometry from each building’s F_{top} , while applying *common* style from the shared $F_{appearance}$ across all of them. As we demonstrate in our experiments (Sec. 4.5), this results in a collection of geometrically diverse buildings that share a cohesive, realistic architectural style, drastically improving scene-level coherence.

Table 1. **Quantitative comparison of 3D urban generation.** ‘‘Top’’ denotes satellite top-view input; ‘‘Front’’ indicates front-view input from the MLLM understanding pipeline.

Method	Top	Front	CD ↓	F ↑	CLIP ↑
TRELLIS	✓	–	0.2803	0.1835	0.7862
Step1x-3D	✓	–	0.2364	0.2073	0.7505
Hunyuan3D-2.1	✓	–	0.1402	0.3650	0.7626
TRELLIS-MV-M	✓	✓	0.0625	0.4699	0.7989
TRELLIS-MV-S	✓	✓	0.0879	0.4727	0.8120
Sat2RealCity (Ours)	✓	✓	0.0138	0.8890	0.8563

3.5. MLLM-powered Semantic-guided Generation Pipeline

We introduce an **MLLM-powered semantic-guided generation pipeline** that bridges satellite imagery and both structure-controllable and appearance-controllable urban generation through multimodal understanding. As illustrated in Figure 2(c), a satellite image is first processed by the *structural prior extraction* module, which retrieves building polygons and height attributes from OSM based on their geographic coordinates.

To capture visual similarities among buildings, we perform a *vision-based clustering* step. Specifically, we employ DINOv3 [37] to extract top-view visual features for each building, resulting in a 1024-dimensional feature vector $\mathbf{v}_i \in \mathbb{R}^{1024}$. The feature is concatenated with the corresponding building height h_i , forming a 1025-dimensional representation $\mathbf{f}_i = [\mathbf{v}_i; h_i] \in \mathbb{R}^{1025}$. These representations are then clustered using HDBSCAN, where buildings within the same cluster are considered to share similar geometric and visual characteristics.

For each cluster, we conduct an *MLLM-based semantic understanding* stage. The top-view images of all buildings in the same cluster are jointly input to the multimodal large language model. The model is guided by a structured prompt that queries for semantic attributes such as building type, exterior color, exterior material, and window layout. The MLLM produces a concise textual description that summarizes the shared visual semantics of that cluster.

Finally, the generated textual descriptions are passed to a *text-to-image* (T2I) model to synthesize corresponding appearance reference images. These generated appearance maps serve as controllable style guidance for the downstream 3D urban generation framework.

4. Experiments

4.1. Implementation details

Our building-entity-based generation model was initialized with the TRELLIS-image-large weights and fine-tuned on our self-constructed 3D building dataset using a learning rate of 0.0001, a batch size of 32, and a total of 40K training

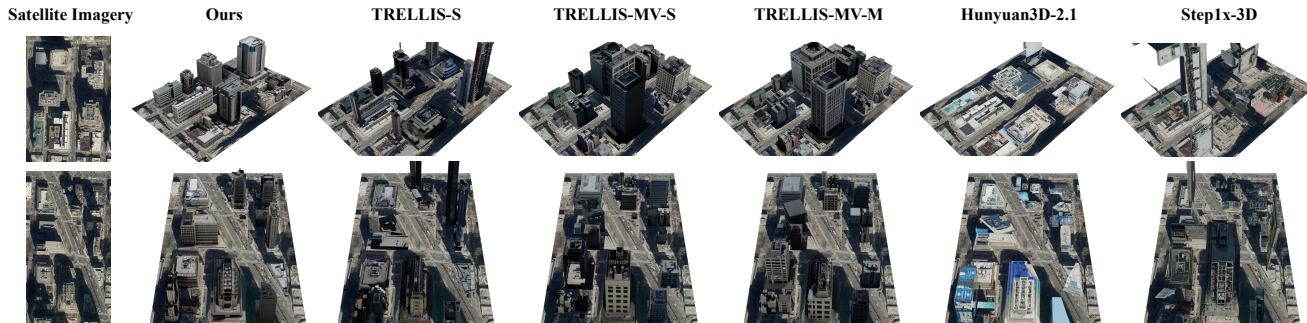


Figure 4. **Qualitative visualization of 3D urban generation.**

steps on 8 NVIDIA A100 GPUs. During training, the OSM-based structural priors module randomly adopted LOD 0 or LOD 1. During inference, satellite imagery and OSM height data were collected from Mapbox and the Overture Maps Foundation, respectively. The clustering module utilized HDBSCAN. The MLLM responsible for generating textual appearance descriptions was implemented using the open-source Qwen3-VL [2, 47], and the model synthesizing building appearances from these descriptions employed the open-source FLUX-dev [15]. Detailed prompts used by both models are provided in the supplementary material. The hyperparameter λ in the OSM-based structural priors module was set to 0.5, and only LOD 1 priors were used.

4.2. Evaluation Data and Metrics

Data. We evaluate our framework on 111 real-world urban regions with high-quality satellite coverage, totaling 10 km^2 . The evaluation covers geometry and appearance. Ground truth data are derived from OSM building footprints with height information for geometry, and from Google Earth Studio city mesh renderings for appearance.

Metrics. To evaluate *geometric consistency*, we compare point clouds from the generated regions against the OSM-based ground truth using the Chamfer Distance (CD) and F-score. CD measures average bidirectional distance, and F-score reflects points within a distance threshold.

For *appearance realism*, we adopt the CLIP Score [32], defined as the cosine similarity between CLIP (ViT-L/14) embeddings of our rendered city views and those of the Google Earth Studio reference. This metric quantifies the perceptual alignment between generated textures and realistic visual appearances.

4.3. Urban Generation

Settings. To our knowledge, this work introduces the first 3D city generation paradigm integrating 3D building entities with satellite-based priors. Based on this, we adapt several advanced 3D object generation models, including TRELIS [43] (single-image version TRELIS and multi-view variant TRELIS-MV). The multi-view variant in-

Table 2. **Quantitative comparison of geometric fidelity.** “Top” denotes the satellite top-view input, while “Front” denotes the front-view input rendered from 3D assets.

Method	Top	Front	CD ↓	F ↑
TRELIS	✓	–	0.0508	0.5778
Step1x-3D	✓	–	0.0230	0.6921
Hunyuan3D-2.1	✓	–	0.0202	0.7099
Sat2RealCity-T (Ours-T)	✓	–	0.0150	0.7871
TRELIS-MV-M	✓	✓	0.0184	0.7929
TRELIS-MV-S	✓	✓	0.0199	0.7763
Sat2RealCity (Ours)	✓	✓	0.0118	0.8554

cludes two strategies: multi-diffusion-based (TRELIS-MV-M) and stochastic sampling (TRELIS-MV-S). We also evaluate Hunyuan3D-2.1 [39] and Step1X-3D [20] under the same building-entity-based setting.

We evaluate all methods on both geometric consistency and appearance realism at the regional level, using the data and metrics introduced in Sec. 4.2. The input condition images for TRELIS-MV include both building rooftop views and appearance guidance images, while other baseline methods use only building rooftop views as input.

Quantitative Results. Table 1 summarizes the results. For *geometric consistency*, our method achieves the lowest CD and highest F-score among baselines, demonstrating superior spatial fidelity. This stems from our OSM-based structural priors explicitly encoding real-world constraints. Baselines lacking pose control tend to produce misaligned or rotated structures. Even after post-hoc rotational registration of all baselines, Sat2RealCity, without correction, achieves higher geometric accuracy, validating the effectiveness of our implicit rotational pose alignment integrated directly into generation.

For *appearance realism*, our model achieves the highest CLIP Score, indicating closest alignment with real-world visuals. This results from our dual-pathway cross-attention, which preserves structural accuracy from satellite priors while incorporating plausible architectural styles

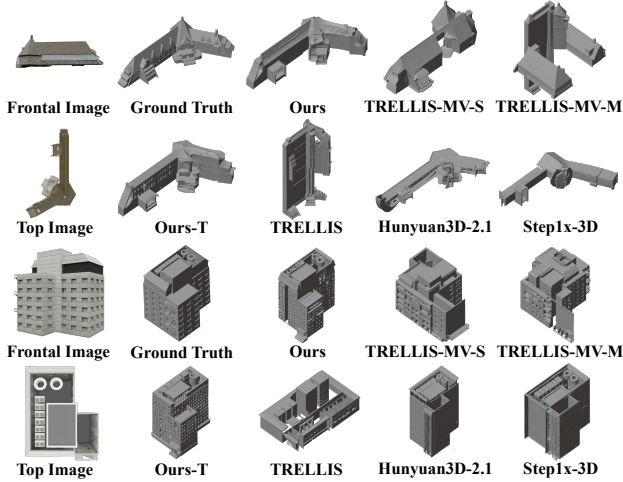


Figure 5. Qualitative visualization of geometric fidelity.

from MLLM-generated appearance conditions. Baselines fail to balance structural control with photorealistic facades, yielding lower visual fidelity.

Qualitative Results. As illustrated in Figure 4, our generated city regions exhibit both precise geospatial alignment and coherent regional style. Buildings are correctly oriented with respect to their OSM footprints and maintain stylistic harmony within each neighborhood. In comparison, baseline results often show inconsistent orientations, distorted roof geometry, or abrupt texture transitions across adjacent buildings. These qualitative observations further corroborate our quantitative findings, demonstrating that Sat2RealCity effectively achieves geometry-faithful and style-consistent regional urban synthesis.

4.4. Ablation Study on Geometric Fidelity

Settings. To further assess the contribution of our OSM-based structural prior to geometric fidelity, we perform controlled ablation experiments on a held-out set of 500 high-quality building assets manually modeled in the City-Craft [5]. Evaluation metrics include CD and F-score, computed between the generated and ground-truth 3D meshes.

Quantitative Results. Table 2 summarizes the results. Sat2RealCity achieves the lowest CD and highest F-score, surpassing TRELLIS-MV even though the latter uses richer multi-view inputs. This demonstrates that explicit structural constraints, rather than simply multi-view information, are essential for precise 3D geometry reconstruction. Importantly, Sat2RealCity-T, which takes the satellite top-view as input, still significantly outperforms other methods. This confirms that the improvement stems from our OSM-based structural prior itself, which effectively resolves geometric ambiguities in single-view satellite imagery.

Qualitative Results. As shown in Figure 5, removing the structural prior leads to noticeable distortions in roof ge-

Table 3. Quantitative comparison of stylistic consistency.

Method	$S_{\text{regional}} \uparrow$
Hunyuan3D-2.0-MV	0.1236
TRELLIS-MV-M	0.3086
TRELLIS-MV-S	0.3027
Sat2RealCity (Ours)	0.7885



Figure 6. Qualitative visualization of stylistic consistency.

ometry and height proportions. In contrast, our method reconstructs sharp, dimensionally consistent structures across diverse building types. These qualitative results further support the quantitative findings, highlighting that the OSM-based prior serves as a strong geometric anchor for single-view 3D generation.

4.5. Ablation Study on Stylistic Consistency

Settings. This experiment validates our *appearance-guided control mechanism*, ensuring stylistic coherence across a region even when individual building geometries differ. From 111 evaluation regions, we selected 20 representative subsets with regional stylistic consistency, where buildings share a unified architectural style but differ in footprint and layout. For each region, a frontal image from our MLLM pipeline served as the *shared style prompt*, and each building was generated from its *unique* satellite top-view input combined with this common appearance condition.

Baselines include multi-view generative models adapted for this setting: TRELLIS-MV and Hunyuan3D-2.0-MV [40], which struggle with geometrically inconsistent inputs (top vs. front views), often overfitting to one modality and losing geometric alignment or stylistic coherence.

To capture this trade-off, we design a composite evaluation framework with two metrics:

- **Structural Alignment (IoU_{top}):** Measures how well generated buildings adhere to satellite footprints. We render the 3D model top-down, binarize it, and compute Intersection-over-Union (IoU) with the ground-truth footprint, averaged over all buildings.
- **Appearance Consistency ($CLIP_{\text{pairwise}}$):** Quantifies stylistic coherence *among* buildings. All N buildings are rendered at 0° elevation, and average CLIP (ViT-L/14) cosine similarity is computed over all unique $\frac{N(N-1)}{2}$ pairs. Finally, the Regional Consistency Score (S_{regional}) is defined as:

$$S_{\text{regional}} = IoU_{\text{top}} \times CLIP_{\text{pairwise}}, \quad (5)$$

Table 4. **Quantitative comparison with city generation methods.**

Method	CLIP \uparrow
CityDreamer	0.7732
Seed3D	0.8167
Sat2RealCity (Ours)	0.8687



Figure 7. **Visual comparison with city generation methods.**

penalizing models failing in geometric fidelity or style uniformity.

Quantitative Results. Table 3 presents the quantitative comparison. Our Sat2RealCity achieves the highest S_{regional} , substantially surpassing all baselines. This demonstrates its superior capability in maintaining coherent regional styles while preserving geometric plausibility across diverse urban scenes.

Qualitative Results. As shown in Figure 6, our generated city regions exhibit coherent architectural styles across buildings with diverse shapes and layouts. Facade materials, color tones, and roof structures remain stylistically consistent while preserving accurate spatial footprints. Baselines often display inconsistent roof orientations or abrupt texture changes across adjacent buildings. These observations confirm that Sat2RealCity achieves region-level stylistic coherence while maintaining high geometric fidelity.

4.6. Comparison with Other City Generation Methods

Settings. Beyond the building-entity-based generation paradigm, we further compare our approach with existing *end-to-end city generation* methods. Since several works such as Sat2City, EarthCrafter, and UrbanWorld have not released implementations, we include two available counterparts: the open-source CityDreamer [45] and the recently released commercial model Seed3D [35].

Considering the supported inference area of these methods, as well as the token limits and usage costs of commercial models, we evaluated an urban region of approximately 1 km^2 from our benchmark for both geometric and appearance assessment. It is worth noting that CityDreamer only outputs rendered RGB frames without explicit 3D geometry, while Seed3D does not support satellite inputs; for it, we provided images of the same region with pitch angles from Google Earth Studio.

Quantitative Results. Due to CityDreamer lacking geometry output and misalignment between our results

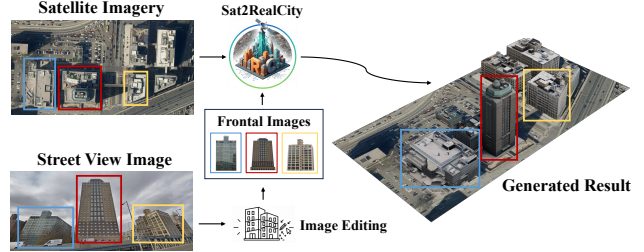


Figure 8. **Extended application with real-world street views.**

and Seed3D, we evaluate appearance, where our method achieves the highest CLIP score, as shown in Table 4. **Qualitative Results.** Figure 7 presents visual comparisons across methods. When conditioned on satellite imagery, our method preserves semantic information consistent with the input. Compared with reference views reconstructed from Google Earth Studio oblique images, our results exhibit superior geometric structure. While Seed3D and CityDreamer produce city layouts that roughly follow urban structure, their outputs lack fine-grained detail and fidelity.

4.7. Extended Applications

While our method currently relies on MLLM-powered semantic-guided appearance control maps during inference, it can be readily extended to incorporate real-world street-view imagery for faithful appearance grounding. To demonstrate this, we used a real-world urban region from satellite imagery and retrieved corresponding street-view images from Google Maps, which serve as ground-truth visual references for building appearances. The generated city results are visualized in Figure 8. The generated buildings exhibit facade appearances consistent with the street-view image, demonstrating the potential of our framework for practical, geographically grounded 3D urban generation.

5. Conclusion

We present Sat2RealCity, a framework for realistic 3D urban generation directly from satellite imagery. Unlike previous city-level methods that rely on large-scale 3D assets or synthetic semantic inputs, Sat2RealCity adopts a building-entity-based paradigm, integrating geometric reasoning, appearance controllability, and semantic guidance. Leveraging OSM-based spatial priors, appearance-guided modeling, and MLLM-powered semantic understanding, our approach achieves fine-grained geometric fidelity and realistic visual synthesis with strong cross-region generalizability. Extensive experiments show that Sat2RealCity outperforms existing city generation methods in both structural coherence and appearance realism, providing interpretable and scalable 3D urban modeling. The framework inherently supports geographically grounded, photorealistic urban scene generation, highlighting its practical potential for real-world applications.

References

- [1] Citydreamer4d: Compositional generative model of unbounded 4d cities. *arXiv e-prints*, pages arXiv–2501, 2025. 3
- [2] Shuai Bai, Keqin Chen, Xuejing Liu, Jialin Wang, Wenbin Ge, Sibao Song, Kai Dang, Peng Wang, Shijie Wang, Jun Tang, Humen Zhong, Yuanzhi Zhu, Mingkun Yang, Zhao-hai Li, Jianqiang Wan, Pengfei Wang, Wei Ding, Zheren Fu, Yiheng Xu, Jiabo Ye, Xi Zhang, Tianbao Xie, Zesen Cheng, Hang Zhang, Zhibo Yang, Haiyang Xu, and Junyang Lin. Qwen2.5-vl technical report. *arXiv preprint arXiv:2502.13923*, 2025. 6
- [3] Jasmine Collins, Shubham Goel, Kenan Deng, Achleshwar Luthra, Leon Xu, Erhan Gundogdu, Xi Zhang, Tomas F Yago Vicente, Thomas Dideriksen, Himanshu Arora, et al. Abo: Dataset and benchmarks for real-world 3d object understanding. In *CVPR*, pages 21126–21136, 2022. 3
- [4] Matt Deitke, Ruoshi Liu, Matthew Wallingford, Huong Ngo, Oscar Michel, Aditya Kusupati, Alan Fan, Christian Laforte, Vikram Voleti, Samir Yitzhak Gadre, Eli VanderBilt, Aniruddha Kembhavi, Carl Vondrick, Georgia Gkioxari, Kiana Ehsani, Ludwig Schmidt, and Ali Farhadi. Objaverse-xl: A universe of 10m+ 3d objects. *arXiv preprint arXiv:2307.05663*, 2023. 3
- [5] Jie Deng, Wenhao Chai, Junsheng Huang, Zhonghan Zhao, Qixuan Huang, Mingyan Gao, Jianshu Guo, Shengyu Hao, Wenhao Hu, Jenq-Neng Hwang, et al. Citycraft: A real crafter for 3d city generation. *arXiv preprint arXiv:2406.04983*, 2024. 1, 2, 7
- [6] Jie Deng, Wenhao Chai, Jianshu Guo, Qixuan Huang, Junsheng Huang, Wenhao Hu, Shengyu Hao, Jenq-Neng Hwang, and Gaoang Wang. Citygen: Infinite and controllable city layout generation. In *CVPR*, pages 1995–2005, 2025. 1, 2
- [7] Huan Fu, Rongfei Jia, Lin Gao, Mingming Gong, Binqiang Zhao, Steve Maybank, and Dacheng Tao. 3d-future: 3d furniture shape with texture. *IJCV*, 129(12):3313–3337, 2021. 3
- [8] Xianglong He, Zi-Xin Zou, Chia-Hao Chen, Yuan-Chen Guo, Ding Liang, Chun Yuan, Wanli Ouyang, Yan-Pei Cao, and Yangguang Li. Sparseflex: High-resolution and arbitrary-topology 3d shape modeling. *arXiv preprint arXiv:2503.21732*, 2025. 2
- [9] Yicong Hong, Kai Zhang, Jiuxiang Gu, Sai Bi, Yang Zhou, Difan Liu, Feng Liu, Kalyan Sunkavalli, Trung Bui, and Hao Tan. Lrm: Large reconstruction model for single image to 3d. *arXiv preprint arXiv:2311.04400*, 2023. 2
- [10] Tongyan Hua, Lutao Jiang, Ying-Cong Chen, and Wufan Zhao. Sat2city: 3d city generation from a single satellite image with cascaded latent diffusion. In *ICCV*, pages 27978–27988, 2025. 1, 2
- [11] Jin Huang, Jantien Stoter, Ravi Peters, and Liangliang Nan. City3d: Large-scale building reconstruction from airborne lidar point clouds. *Remote Sensing*, 14(9):2254, 2022. 3
- [12] Zhangyu Jin and Andrew Feng. Sat-skylines: 3d building generation from satellite imagery and coarse geometric priors. *arXiv preprint arXiv:2508.18531*, 2025. 4
- [13] Bernhard Kerbl, Georgios Kopanas, Thomas Leimkühler, and George Drettakis. 3d gaussian splatting for real-time radiance field rendering. *ACM Trans. Graph.*, 42(4):139–1, 2023. 2
- [14] Mukul Khanna, Yongsen Mao, Hanxiao Jiang, Sanjay Haresh, Brennan Shacklett, Dhruv Batra, Alexander Clegg, Eric Undersander, Angel X Chang, and Manolis Savva. Habitat synthetic scenes dataset (hssd-200): An analysis of 3d scene scale and realism tradeoffs for objectgoal navigation. In *CVPR*, pages 16384–16393, 2024. 3
- [15] Black Forest Labs, Stephen Batifol, Andreas Blattmann, Frederic Boesel, Saksham Consul, Cyril Diagne, Tim Dockhorn, Jack English, Zion English, Patrick Esser, et al. Flux. 1 kontext: Flow matching for in-context image generation and editing in latent space. *arXiv preprint arXiv:2506.15742*, 2025. 6
- [16] Zeqiang Lai, Yunfei Zhao, Haolin Liu, Zibo Zhao, Qingxiang Lin, Huiwen Shi, Xianghui Yang, Mingxin Yang, Shuhui Yang, Yifei Feng, et al. Hunyuan3d 2.5: Towards high-fidelity 3d assets generation with ultimate details. *arXiv preprint arXiv:2506.16504*, 2025. 2, 4
- [17] Zeqiang Lai, Yunfei Zhao, Zibo Zhao, Haolin Liu, Fuyun Wang, Huiwen Shi, Xianghui Yang, Qingxiang Lin, Jingwei Huang, Yuhong Liu, et al. Unleashing vecset diffusion model for fast shape generation. *arXiv preprint arXiv:2503.16302*, 2025. 2
- [18] Han-Hung Lee, Qinghong Han, and Angel X Chang. Nuiscene: Exploring efficient generation of unbounded outdoor scenes. *arXiv preprint arXiv:2503.16375*, 2025. 3
- [19] Weiyu Li, Jiarui Liu, Hongyu Yan, Rui Chen, Yixun Liang, Xuelin Chen, Ping Tan, and Xiaoxiao Long. Craftsman3d: High-fidelity mesh generation with 3d native generation and interactive geometry refiner. *arXiv preprint arXiv:2405.14979*, 2024. 2
- [20] Weiyu Li, Xuanyang Zhang, Zheng Sun, Di Qi, Hao Li, Wei Cheng, Weiwei Cai, Shihao Wu, Jiarui Liu, Zihao Wang, et al. Step1x-3d: Towards high-fidelity and controllable generation of textured 3d assets. *arXiv preprint arXiv:2505.07747*, 2025. 6
- [21] Yangguang Li, Zi-Xin Zou, Zexiang Liu, Dehu Wang, Yuan Liang, Zhipeng Yu, Xingchao Liu, Yuan-Chen Guo, Ding Liang, Wanli Ouyang, et al. Triposg: High-fidelity 3d shape synthesis using large-scale rectified flow models. *arXiv preprint arXiv:2502.06608*, 2025. 2
- [22] Zuoyue Li, Zhenqiang Li, Zhaopeng Cui, Marc Pollefeys, and Martin R Oswald. Sat2scene: 3d urban scene generation from satellite images with diffusion. In *CVPR*, pages 7141–7150, 2024. 1, 2
- [23] Liqiang Lin, Yilin Liu, Yue Hu, Xingguang Yan, Ke Xie, and Hui Huang. Capturing, reconstructing, and simulating: the urbanscene3d dataset. In *European Conference on Computer Vision*, pages 93–109. Springer, 2022. 3
- [24] Minghua Liu, Ruoxi Shi, Linghao Chen, Zhuoyang Zhang, Chao Xu, Xinyue Wei, Hansheng Chen, Chong Zeng, Jiayuan Gu, and Hao Su. One-2-3-45++: Fast single image to 3d objects with consistent multi-view generation and 3d diffusion. In *CVPR*, pages 10072–10083, 2024. 2

- [25] Ruoshi Liu, Rundi Wu, Basile Van Hoorick, Pavel Tokmakov, Sergey Zakharov, and Carl Vondrick. Zero-1-to-3: Zero-shot one image to 3d object. In *ICCV*, pages 9298–9309, 2023. 1, 2
- [26] Shang Liu, Chenjie Cao, Chaohui Yu, Wen Qian, Jing Wang, and Fan Wang. Earthcrafter: Scalable 3d earth generation via dual-sparse latent diffusion. *arXiv preprint arXiv:2507.16535*, 2025. 1, 2
- [27] Xinhang Liu, Chi-Keung Tang, and Yu-Wing Tai. Worldcraft: Photo-realistic 3d world creation and customization via llm agents. *arXiv preprint arXiv:2502.15601*, 2025. 1
- [28] Fan Lu, Kwan-Yee Lin, Yan Xu, Hongsheng Li, Guang Chen, and Changjun Jiang. Urban architect: Steerable 3d urban scene generation with layout prior. *arXiv preprint arXiv:2404.06780*, 2024. 1
- [29] Ben Mildenhall, Pratul P Srinivasan, Matthew Tancik, Jonathan T Barron, Ravi Ramamoorthi, and Ren Ng. Nerf: Representing scenes as neural radiance fields for view synthesis. *Communications of the ACM*, 65(1):99–106, 2021. 2
- [30] Maxime Oquab, Timothée Darcet, Théo Moutakanni, Huy Vo, Marc Szafraniec, Vasil Khalidov, Pierre Fernandez, Daniel Haziza, Francisco Massa, Alaaeldin El-Nouby, et al. Dinov2: Learning robust visual features without supervision. *arXiv preprint arXiv:2304.07193*, 2023. 2, 5
- [31] Ben Poole, Ajay Jain, Jonathan T Barron, and Ben Mildenhall. Dreamfusion: Text-to-3d using 2d diffusion. *arXiv preprint arXiv:2209.14988*, 2022. 1, 2
- [32] Alec Radford, Jong Wook Kim, Chris Hallacy, Aditya Ramesh, Gabriel Goh, Sandhini Agarwal, Girish Sastry, Amanda Askell, Pamela Mishkin, Jack Clark, et al. Learning transferable visual models from natural language supervision. In *ICML*, pages 8748–8763. PmlR, 2021. 6
- [33] Xuanchi Ren, Jiahui Huang, Xiaohui Zeng, Ken Museth, Sanja Fidler, and Francis Williams. Xcube: Large-scale 3d generative modeling using sparse voxel hierarchies. In *CVPR*, pages 4209–4219, 2024. 2
- [34] Robin Rombach, Andreas Blattmann, Dominik Lorenz, Patrick Esser, and Björn Ommer. High-resolution image synthesis with latent diffusion models. In *CVPR*, pages 10684–10695, 2022. 1
- [35] ByteDance Seed. Seed3d 1.0: From images to high-fidelity simulation-ready 3d assets. 8
- [36] Yu Shang, Yuming Lin, Yu Zheng, Hangyu Fan, Jingtao Ding, Jie Feng, Jiasheng Chen, Li Tian, and Yong Li. Urbanworld: An urban world model for 3d city generation. *arXiv preprint arXiv:2407.11965*, 2024. 1, 2
- [37] Oriane Siméoni, Huy V Vo, Maximilian Seitzer, Federico Baldassarre, Maxime Oquab, Cijo Jose, Vasil Khalidov, Marc Szafraniec, Seungeun Yi, Michaël Ramamonjisoa, et al. Dinov3. *arXiv preprint arXiv:2508.10104*, 2025. 5
- [38] Jiayang Tang, Zhaoxi Chen, Xiaokang Chen, Tengfei Wang, Gang Zeng, and Ziwei Liu. Lgm: Large multi-view gaussian model for high-resolution 3d content creation. In *ECCV*, pages 1–18. Springer, 2024. 2
- [39] Tencent Hunyuan3D Team. Hunyuan3d 2.1: From images to high-fidelity 3d assets with production-ready pbr material, 2025. 2, 6
- [40] Tencent Hunyuan3D Team. Hunyuan3d 2.0: Scaling diffusion models for high resolution textured 3d assets generation, 2025. 2, 7
- [41] Ruisheng Wang, Shangfeng Huang, and Hongxin Yang. Building3d: A urban-scale dataset and benchmarks for learning roof structures from point clouds. In *ICCV*, pages 20076–20086, 2023. 3
- [42] Congcong Wen, Wenyu Han, Lazarus Chok, Yan Liang Tan, Sheung Lung Chan, Hang Zhao, and Chen Feng. Reality3d: A large-scale georeferenced 3d shape dataset of real-world cities. 3
- [43] Jianfeng Xiang, Zelong Lv, Sicheng Xu, Yu Deng, Ruicheng Wang, Bowen Zhang, Dong Chen, Xin Tong, and Jiaolong Yang. Structured 3d latents for scalable and versatile 3d generation. In *CVPR*, pages 21469–21480, 2025. 1, 2, 3, 4, 5, 6
- [44] Enze Xie, Junsong Chen, Junyu Chen, Han Cai, Haotian Tang, Yujun Lin, Zhekai Zhang, Muyang Li, Ligeng Zhu, Yao Lu, et al. Sana: Efficient high-resolution image synthesis with linear diffusion transformers. *arXiv preprint arXiv:2410.10629*, 2024. 1
- [45] Haozhe Xie, Zhaoxi Chen, Fangzhou Hong, and Ziwei Liu. Citydreamer: Compositional generative model of unbounded 3d cities. In *CVPR*, pages 9666–9675, 2024. 1, 8
- [46] Jiale Xu, Weihao Cheng, Yiming Gao, Xintao Wang, Shenghua Gao, and Ying Shan. Instantmesh: Efficient 3d mesh generation from a single image with sparse-view large reconstruction models. *arXiv preprint arXiv:2404.07191*, 2024. 2
- [47] An Yang, Anfeng Li, Baosong Yang, Beichen Zhang, Binyuan Hui, Bo Zheng, Bowen Yu, Chang Gao, Chengen Huang, Chenxu Lv, et al. Qwen3 technical report. *arXiv preprint arXiv:2505.09388*, 2025. 6
- [48] Xianghui Yang, Huiwen Shi, Bowen Zhang, Fan Yang, Jiacheng Wang, Hongxu Zhao, Xinhai Liu, Xinzhou Wang, Qingxiang Lin, Jiao Yu, et al. Hunyuan3d 1.0: A unified framework for text-to-3d and image-to-3d generation. *arXiv preprint arXiv:2411.02293*, 2024. 2
- [49] Biao Zhang, Jiapeng Tang, Matthias Niessner, and Peter Wonka. 3dshape2vecset: A 3d shape representation for neural fields and generative diffusion models. *TOG*, 42(4):1–16, 2023. 1, 2
- [50] Kai Zhang, Sai Bi, Hao Tan, Yuanbo Xiangli, Nanxuan Zhao, Kalyan Sunkavalli, and Zexiang Xu. Gs-irm: Large reconstruction model for 3d gaussian splatting. In *ECCV*, pages 1–19. Springer, 2024. 2
- [51] Lvmin Zhang, Anyi Rao, and Maneesh Agrawala. Adding conditional control to text-to-image diffusion models. In *ICCV*, pages 3836–3847, 2023. 1
- [52] Longwen Zhang, Ziyu Wang, Qixuan Zhang, Qiwei Qiu, Anqi Pang, Haoran Jiang, Wei Yang, Lan Xu, and Jingyi Yu. Clay: A controllable large-scale generative model for creating high-quality 3d assets. *TOG*, 43(4):1–20, 2024. 2
- [53] Shougao Zhang, Mengqi Zhou, Yuxi Wang, Chuanchen Luo, Rongyu Wang, Yiwei Li, Zhaoxiang Zhang, and Junran Peng. Cityx: Controllable procedural content generation for unbounded 3d cities. *arXiv preprint arXiv:2407.17572*, 2024. 2